Caspase-dependent apoptotic death by gadolinium chloride ($GdCl_3$) via reactive oxygen species production and MAPK signaling in rat C6 glioma cells

YUH-FENG TSAI[1,2], YUH-FUNG CHEN[3], CHEN-YU HSIAO[1], CHING-WEN HUANG[1], CHI-CHENG LU[4], SHIH-CHANG TSAI[5] and JAI-SING YANG[6]

[1]Department of Diagnostic Radiology, Shin-Kong Wu Ho-Su Memorial Hospital, Taipei 111; [2]School of Medicine, Fu-Jen Catholic University, New Taipei 202; [3]Department of Pharmacology, School of Medicine, China Medical University; [4]Department of Sport Performance, National Taiwan University of Sport; [5]Department of Biological Science and Technology; [6]Department of Medical Research, China Medical University Hospital, China Medical University, Taichung 404, Taiwan, R.O.C.

Received July 16, 2018; Accepted November 21, 2018

DOI: 10.3892/or.2018.6913

Abstract. Gadolinium (Gd) compounds serve as magnetic resonance imaging contrast agents and exert certain anticancer activities. Yet, the molecular signaling underlying the antitumor effect of Gd chloride ($GdCl_3$) on glioma remains unclear. In the present study, we aimed to ascertain the apoptotic mechanisms of $GdCl_3$ on rat glioma C6 cells. Our results demonstrated that $GdCl_3$ significantly reduced cell viability and shrunk cell morphology of C6 cells in a concentration-dependent manner. $GdCl_3$ led to apoptotic C6 cell death as detected by TUNEL staining. An increase in cleaved caspase-3, cleaved caspase-8 and cleaved caspase-9 occurred in $GdCl_3$-treated C6 cells as detected by immunoblotting analysis. The activities of caspase-3, caspase-8 and caspase-9 were increased, and the specific inhibitors of caspase-3/-8/-9 individually reversed cell viability, which caused apoptotic death in C6 cells prior to $GdCl_3$ exposure. $GdCl_3$ also caused an elevation in the cytoplasmic Ca^{2+} level and reactive oxygen species (ROS) production, as well as the loss of mitochondrial membrane potential ($\Delta\Psi m$) as shown by flow cytometric analysis in C6 cells. The results from the immunoblotting analysis demonstrated that there were upregulated protein levels of cytochrome *c* and Bax but a downregulated protein level of Bcl-2 in C6 cells after $GdCl_3$ treatment. Additionally, $GdCl_3$ decreased the protein levels of phosphorylated-extracellular signal-regulated kinases, phosphorylated-c-Jun N-terminal kinase and phosphorylated-p38 mitogen-activated protein kinases in C6 cells. In conclusion, ROS production and MAPKs signaling pathways contribute to $GdCl_3$-induced caspase cascade-mediated apoptosis in C6 cells. Our findings provide a better understanding of the molecular mechanisms underlying the role of $GdCl_3$ in rat glioma C6 cells.

Introduction

Glioma is characterized as a malignant brain tumor with a high recurrence rate, and surgery is utilized to remove the tumor (1,2). However, patients with glioma have a high mortality rate and an extremely poor prognosis (2). Currently, chemotherapy is the main method for prolonging survival or reducing symptoms (3,4). It is known that the existence of the blood-tumor barrier (BTB) in tumor tissue limits the efficacy and the delivery of therapeutic agents to brain tumor tissue (1,3). Therefore, the development of therapeutic agents to pass through the BTB is increasingly needed to effectively limit the rapid and invasive growth of malignant gliomas (5,6).

Lanthanide (Ln) ions have the chemical properties of both a high coordination number and a charge density, and they have been previously applied in agriculture and medicine (7-12). Gadolinium (Gd), a member of the Ln series, exerts a magneto-caloric effect (8). Gd compounds including Gd chloride ($GdCl_3$) have been applied as magnetic resonance imaging (MRI) contrast agents and may be promising anticancer drugs (8-12). $GdCl_3$ is widely used for in-activating tumor-associated macrophages (9,13). In addition, $GdCl_3$ was found to inhibit cell proliferation and induce apoptosis in human hepatoma HepG2 cells through a mitochondria-dependent pathway (11). Recently, we reported that $GdCl_3$ triggers apoptotic death in human osteosarcoma U-2 OS cells through the death receptor, mitochondria-dependent and ER stress pathways (8). The exact molecular mechanism of $GdCl_3$ that

Correspondence to: Dr Jai-Sing Yang, Department of Medical Research, China Medical University Hospital, China Medical University, 2 Yude Road, Taichung 40447, Taiwan, R.O.C.
E-mail: jaisingyang@gmail.com

Dr Shih-Chang Tsai, Department of Biological Science and Technology, China Medical University, 91 Hsueh-Shih Road, Taichung 40402, Taiwan, R.O.C.
E-mail: sctsai@mail.cmu.edu.tw

Key words: gadolinium chloride, $GdCl_3$, apoptosis, reactive oxygen species production, MAPK pathway, caspase cascade

underlie the inhibition of the viability of rat C6 glioma cells remains undefined. Therefore, the present study aimed to investigate the effect of $GdCl_3$ on rat C6 glioma cells and the possible mechanism of $GdCl_3$-induced apoptosis.

Materials and methods

Chemicals and reagents. Fetal bovine serum (FBS), L-glutamine, penicillin/streptomycin, trypsin-EDTA, and Ham's Nutrient Mixture F12 medium were obtained from HyClone; GE Healthcare Life Sciences (Logan, UT, USA). $GdCl_3$, 3-(4,5-dimethylthiazol-2-yl)-2,5-diphenyltetrazolium bromide (MTT), 4',6-diamidino-2-phenylindole (DAPI), propidium iodide (PI), and *In Situ* Cell Death Detection kit, Fluorescein were obtained from Sigma-Aldrich; Merck KGaA (Darmstadt, Germany). Z-VAD-FMK (a pan-caspase inhibitor), Z-DEVD-FMK (a caspase-3 inhibitor), Z-IETD-FMK (a caspase-8 inhibitor), Z-LEHD-FMK (a caspase-9 inhibitor) and Caspase-3/-8/-9 Colorimetric Assay kits were purchased from R&D Systems, Inc. (Minneapolis, MN, USA). All primary antibodies against caspase-3 (cat. no. GTX110543), caspase-8 (cat. no. GTX110723), caspase-9 (cat. no. GTX112888), cytochrome *c* (cat. no. GTX108585), Bax (cat. no. GTX109683), Bcl-2 (cat. no. GTX100064), phosphorylated-extracellular signal-regulated kinase (p-ERK) (cat no. GTX59568), ERK (cat no. GTX59618), phosphorylated-c-Jun N-terminal kinase (p-JNK) (cat no. GTX52326), JNK (cat no. GTX52360), phosphorylated-p38 (p-p38) (cat no. GTX24822), p38 (cat no. GTX110720), β-actin (cat. no. GTX109639), as well as anti-mouse (cat. no. GTX213111-01) and anti-rabbit (cat. no. GTX213110-01) immunoglobulin (Ig) G horseradish peroxidase (HRP)-linked secondary antibodies were purchased from GeneTex International Corporation (Hsinchu, Taiwan). Dihydrorhodamine 123, 3,3'-dihexyloxacarbocyanine iodide [$DiOC_6(3)$] and Fluo-3/AM were sourced from Thermo Fisher Scientific, Inc. (Waltham, MA, USA).

Cell culture. Rat glial cell tumor C6 cell line was obtained from the Bioresource Collection and Research Center (BCRC; Hsinchu, Taiwan) and cultured in 75-cm^2 flasks with Ham's Nutrient Mixture F12 medium supplemented with 10% FBS, 2 mM L-glutamine, 100 U/ml penicillin, and 100 μg/ml streptomycin. Human fetal glial SVG p12 cell line was purchased from BCRC and cultured in minimum essential Eagle's medium containing 10% FBS, 0.1 mM non-essential amino acids, 1.0 mM sodium pyruvate, 100 U/ml penicillin, and 100 μg/ml streptomycin. All cells were maintained in a humidified incubator at 37˚C with 5% CO_2.

Cell viability assay and morphological observation. Cell viability was determined by a colorimetric MTT assay, as previously described (14). Briefly, C6 and SVG p12 cells ($1x10^4$ cells/100 μl) in a 96-well plate were incubated at 37˚C with or without $GdCl_3$ at a final concentration of 50, 100, 150 and 200 μM for 24 h. After incubation, the medium was removed, and the cells were mixed with 0.5 mg/ml MTT solution for 4 h. The insoluble formazan crystals were dissolved in 0.1 ml dimethyl sulfoxide (DMSO) for 30 min at 37˚C. The absorbance was spectrophotometrically measured with an ELISA reader at a wavelength of 570 nm. The result was calculated as a ratio of sample absorbance to the control (vehicle) absorbance, considered as 100%. Additionally, the $GdCl_3$-treated C6 cells were measured for apoptotic characteristics and photographed via a phase-contrast microscope, as previously described (14).

DNA breaks for apoptosis. C6 cells ($1x10^5$ cells/ml) were exposed to 50, 100, and 150 μM of $GdCl_3$ for 24 h. The cells were subsequently collected and stained with the *In Situ* Cell Death Detection kit, Fluorescein (Sigma-Aldrich; Merck KGaA), following the manufacturer's instructions. The terminal deoxynucleotidyl transferase-mediated d-UTP nick end labeling (TUNEL)-positive cells were detected by flow cytometry (BD FACSCalibur flow cytometer; BD Biosciences, Franklin Lakes, San Jose, CA, USA), as previously described (14).

Comet assay and DAPI staining. C6 cells ($2x10^5$ cells/well) were treated with 0, 50, 100, 150 and 200 μM of $GdCl_3$ for 24 h. Comet assay was applied according to the vendor's instructions and a previous study (15). Additionally, chromatin undergoes a phase change from loose to condensed during apoptosis. DAPI dye was used to observe condensed chromatin, as previously described (16).

Immunoblotting analysis. C6 cells ($5x10^6$ cells/75T flask) were incubated with the presence and absence of 0, 50, 100 and 200 μM of $GdCl_3$ for 24 h. After cells were lysed, total protein (40 μg) was separated using 10% SDS-polyacrylamide gel electrophoresis (PAGE) and transferred onto polyvinylidene difluoride (PVDF) membranes (Immobilon-P Transfer membrane; Merck Millipore, Darmstadt, Germany). As previously described (17,18), the membranes were probed with primary antibodies against caspase-3, caspase-8, caspase-9, cytochrome *c*, Bax, Bcl-2, p-ERK, ERK, p-JNK, JNK, p-p38, p38, (all 1:1,000 dilution) and β-actin (1:5,000 dilution). The membranes were then incubated with goat anti-rabbit IgG-HRP or goat anti-mouse IgG-HRP linked antibodies (1:10,000 dilution) for 1 h at room temperature. All immunoblots were hybridized using an Enhanced Chemiluminescence system kit (Immobilon Western Chemiluminescent HRP substrate; Merck Millipore). The intensity of relative protein expression was normalized to β-actin signal and quantified with the NIH ImageJ program (version 1.47; National Institutes of Health, Bethesda, MD, USA).

Assays for caspase-3/-8/-9 activities. C6 cells ($5x10^6$ cells/75T flask) were exposed to 0, 50, 100, and 200 μM of $GdCl_3$ for 24 h. The cell lysates were then harvested and incubated with a commercial lysis buffer according to the instructions of the manufacturer (Caspase-3,-8 and -9 Colorimetric Assay kits; R&D Systems).

Determinations of reactive oxygen species (ROS), the mitochondrial membrane potential ($\Delta\Psi m$) and intracellular Ca^{2+} levels via flow cytometry. C6 cells ($2x10^5$ cells/well) were incubated with or without 50, 100, 150 and 200 μM of $GdCl_3$ for 6 h. After treatment, the medium was replaced with 5 μM dihydrorhodamine 123 (an ROS indicator), 4 nM DiOC6(3) (a $\Delta\Psi m$ fluorescent probe) and 3 μg/ml Fluo-3/AM (cytoplasmic

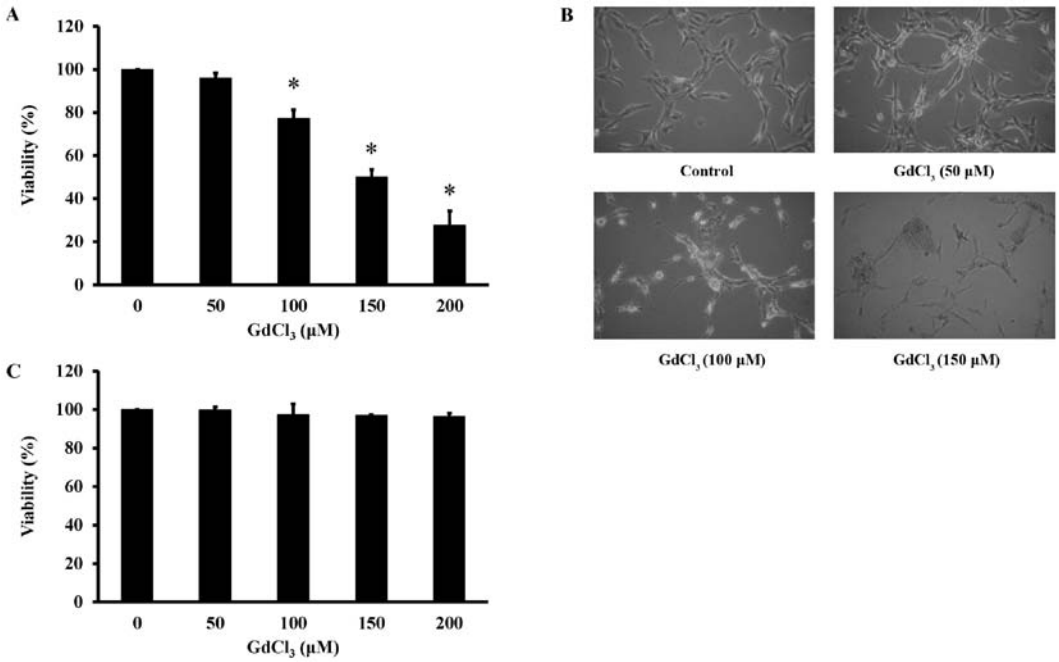

Figure 1. Effects of $GdCl_3$ on the cell viability of rat glioma C6 and human normal fetal glial SVG p12 cells. (A) Viability of C6 cells treated with $GdCl_3$ at the indicated concentrations for 24 h via an MTT assay. Data are expressed as the mean ± SD (n=3). *P<0.05 compared to the control. (B) Morphological changes of C6 cells treated with $GdCl_3$ at 50, 100, and 150 μM of $GdCl_3$ for 24 h. Images were taken from one of three independent experiments; (magnification, x200). (C) SVG p12 cells were exposed to $GdCl_3$ (0, 50, 100, 150, and 200 μM) for 24 h. Cell viability was determined via an MTT method. $GdCl_3$, gadolinium chloride; SD, standard deviation.

Ca^{2+} dye), respectively, and the plates were protected from light for 30 min at 37˚C. The mean fluorescence intensity (MFI) was measured via flow cytometry (Muse Cell Analyzer; Merck Millipore) and expressed as % of the control (vehicle), as previously described (14,19).

Statistical analysis. All data are represented as the mean ± standard deviation (SD) from at least three independent experiments. Statistical calculations of the data were carried out via one-way analysis of variance (ANOVA) followed by Dunnett's test using SPSS software version 16.0 (SPSS, Inc., Chicago, IL, USA). P<0.05 was considered to indicate a statistically significant difference.

Results

$GdCl_3$ inhibits viability of rat C6 glioma cells. The MTT assay was used to evaluate the impact of $GdCl_3$ on C6 cells. The cells were treated with $GdCl_3$ at the different concentrations (0, 50, 100, 150, and 200 μM) for 24 h. The cell viability was significantly decreased with the treatment of >100 μM $GdCl_3$ in a concentration-dependent manner (Fig. 1A). The half-maximal inhibitory concentration (IC_{50}) of $GdCl_3$ for C6 cells was 152.36±2.45 μM. $GdCl_3$ at the concentration of 150 μM markedly caused apoptotic cell shrinkage and the morphological changes, but the untreated control was well spread in C6 cells (Fig. 1B). Our results suggested that $GdCl_3$ possessed a cytotoxic effect on C6 cells. However, no effect of viability (Fig. 1C) and morphological change (data not shown) was observed on normal SVG p12 cells after $GdCl_3$ treatment (0, 50, 100, 150, and 200 μM). Therefore, $GdCl_3$ may exhibit lower toxicity in normal glial SVG p12 cells.

$GdCl_3$ induces apoptosis in C6 cells. To explore whether $GdCl_3$ induces C6 cell death through an apoptotic mechanism, a TUNEL assay was used to detect DNA breaks in apoptotic cells. The percentage of TUNEL-positive cells (cells undergoing apoptosis) was markedly increased in $GdCl_3$-treated C6 cells compared to that noted in the control cells, and the effect was concentration-dependent (Fig. 2A). We also measured DNA damage using comet assay. $GdCl_3$ triggered DNA damage through the production of a longer comet tail (Fig. 2B, upper panel) after DNA was stained with PI in C6 cells. Moreover, chromatin and apoptotic DNA condensation was observed in C6 cells after $GdCl_3$ exposure using DAPI staining (Fig. 2B, bottom panel). Our findings indicate that $GdCl_3$ provoked an apoptotic response in C6 cells.

GdCl3 elevates the activities of caspase-3, caspase-8 and caspase-9 in C6 cells. To characterize the mechanism of $GdCl_3$-induced apoptosis, we explored the expression levels of caspase-3, caspase-8 and caspase-9 using immunoblotting analysis. $GdCl_3$ increased cleaved caspase-3, cleaved caspase-8 and cleaved caspase-9 levels in C6 cells (Fig. 3A). We also examined the activities of caspase-3, caspase-8 and caspase-9 in $GdCl_3$-treated C6 cells. The activities of caspase-3 (Fig. 3B), caspase-8 (Fig. 3C) and caspase-9 (Fig. 3D) were elevated after $GdCl_3$ challenge, and the effects were concentration-dependent. Furthermore, the cells were pre-treated with a pan-caspase inhibitor (Z-VAD-FMK) (Fig. 4A), and selective inhibitors to caspase-3, caspase-8 and caspase-9 (Fig. 4B) to confirm the specificities of caspases. Data showed that specific inhibitors to caspase-3 (Z-DEVD-FMK), caspase-8 (Z-IETD-FMK) and caspase-9 (Z-LEHD-FMK) significantly prevented the $GdCl_3$-reduced cell viability (Fig. 4B). These data suggest

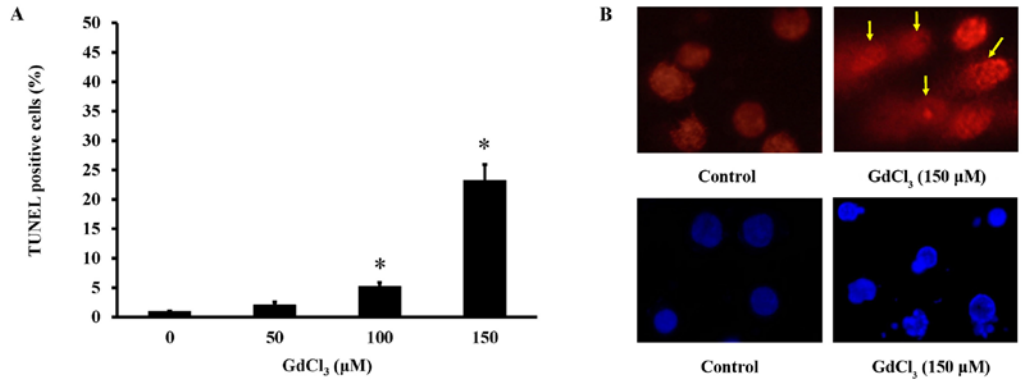

Figure 2. Effects of $GdCl_3$ on the apoptosis of rat glioma C6 cells. (A) Cells were treated with $GdCl_3$ at indicated concentrations for 24 h. Apoptotic cells were determined by TUNEL assay kit, as described in Materials and methods. Data are presented as the mean ± SD (n=3). *P<0.05 compared to the control. (B) Fluorescence staining of apoptotic cells in $GdCl_3$-treated cells were observed. PI was used to stain the nuclei via comet assay (upper panel), and the yellow arrows indicate the nuclei and DNA damage of apoptotic cells. DAPI dye was applied to probe the nuclei condensation (bottom panel); x400 magnification. Representative images are from one of three independent experiments. $GdCl_3$, gadolinium chloride; PI, propidium iodide.

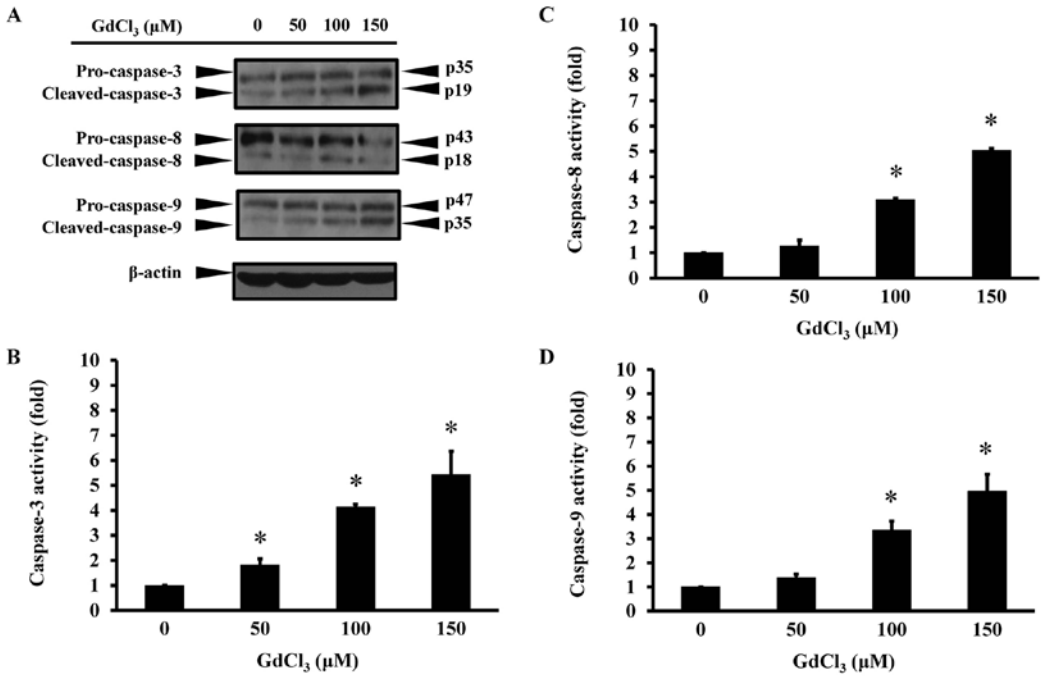

Figure 3. Effects of $GdCl_3$ on caspase cascade protein expression and activities in rat glioma C6 cells. Cells were treated with 50, 100, and 150 μM of $GdCl_3$ for 24 h. The cell lysates were harvested to assess (A) the expression levels of caspase-3, caspase-8, and caspase-9 using immunoblotting analysis. β-actin was used as a control to ensure an equal loading amount. Representative chemiluminescent images were collected from one of independent duplicate experiments. The activities of (B) caspase-3, (C) caspase-8, and (D) caspase-9 were monitored, as described in Materials and methods. Data are presented as the mean ± SD (n=3). *P<0.05 compared to the control. $GdCl_3$, gadolinium chloride; SD, standard deviation.

that the caspase cascade-mediated the signaling results in $GdCl_3$-induced apoptosis in C6 cells.

$GdCl_3$ enhances the ROS production and loss of ΔΨm level in C6 cells. To detect the effect of $GdCl_3$ on ROS production in C6 cells, we measured intracellular ROS levels by dihydrorhodamine 123 fluorescent dye, and the stained cells were analyzed by flow cytometry. Intracellular ROS levels were concentration-dependently increased in C6 cells following $GdCl_3$ exposure (Fig. 5A). To further test the effect of $GdCl_3$ on ΔΨm levels, we used the specific fluorescent probe DiOC6(3) to detect the levels of ΔΨm. $GdCl_3$ disrupted the ΔΨm level in C6 cells, and this impact was in a concentration-dependent manner (Fig. 5B). These results indicate that $GdCl_3$ triggered apoptosis via ROS production and mitochondrial dysfunction in C6 cells.

$GdCl_3$ prompts cytoplasmic Ca^{2+} level in C6 cells. To further elucidate whether the Ca^{2+} level is involved in $GdCl_3$-induced apoptosis and the possible signaling in C6 cells, we detected intracellular Ca^{2+} levels by flow cytometric analysis. The cells were treated with 50, 100, and 150 μM of $GdCl_3$ for 24 h. $GdCl_3$ significantly increased the intracellular Ca^{2+} level (Fig. 5C). These results revealed that cytoplasmic Ca^{2+} signaling and ER stress-mediated pathway may contribute to $GdCl_3$-induced apoptotic machinery in C6 cells.

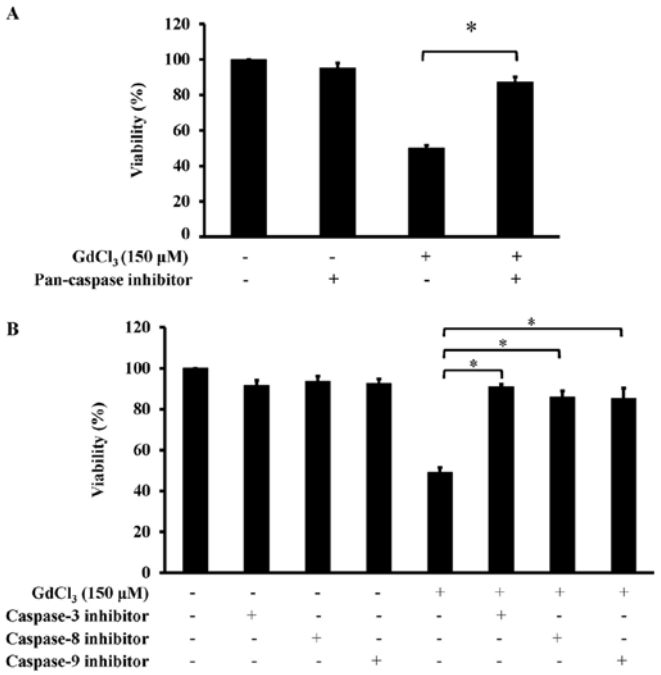

Figure 4. Effects of caspase inhibitors to reverse $GdCl_3$-reduced viability of rat glioma C6 cells. Cells were treated with 150 μM $GdCl_3$ for 24 h after being pre-incubated with or without (A) 15 μM Z-VAD-FMK (a pan-caspase inhibitor) and (B) 15 μM Z-DEVD-FMK (a caspase-3 inhibitor), Z-IETD-FMK (a caspase-8 inhibitor), and Z-LEHD-FMK (a caspase-9 inhibitor) for 2 h, respectively. Cell viability was determined by the MTT assay. Data are expressed as the mean ± SD (n=3). $^*P<0.05$ compared to the control. $GdCl_3$, gadolinium chloride; SD, standard deviation.

$GdCl_3$ alters the levels of apoptosis- and mitogen-activated protein kinase (MAPK)-related protein molecules in C6 cells. To understand the molecular mechanisms of the apoptotic pathway, we further explored the levels of apoptosis-related protein signals (cytochrome *c*, Bax and Bcl-2) using immunoblotting analysis. The levels of cytochrome *c* and Bax were increased. By contrast, the level of anti-apoptotic protein Bcl-2 was decreased in $GdCl_3$-treated cells (Fig. 5D). In addition, we also investigated the levels of MAPK-related pathway proteins (p-ERK, ERK, p-JNK, JNK, p-p38 MAPK and p38 MAPK) also using immunoblotting analysis. $GdCl_3$ downregulated the levels of the p-ERK, p-JNK and p-p38 MAPK pathway in C6 cells (Fig. 6). These data demonstrated that $GdCl_3$-induced apoptotic cell death may result from mitochondria-dependent and MAPK-mediated signaling in C6 cells.

Discussion

Malignant glioma is an invasive intracranial tumor that grows rapidly and has extremely high recurrence (1,20). At present, postoperative chemotherapy has become a powerful strategy for the treatment of adult glioma patients (1,2,20). However, treatment has been particularly inefficient for glioma patients administered chemotherapeutic agents due to the existence of the BTB. The permeability of the BTB and blood brain barrier (BBB) impedes the accumulation and uptake rate of potential drugs to brain tumor tissues (1,2,20). Liu *et al* (21) showed that the efficacy of killing brain tumor cells increased by 10-fold when the therapeutic agent was permeabilized into the area of the brain tumor tissue. Hopefully, a therapeutic agent can be found that can pass through the BTB and BBB, and with that the efficacy of chemotherapy in treating glioma would be markedly improved. Gd-based contrast agents (GBCAs) are applied as pharmaceuticals and have been approved for 30 years and are used daily in millions of patients worldwide (22). In recent years, numerous retrospective clinical studies have reported the unexpected long-term presence of Gd in the brain after receiving radiology practice (22,23). Previous studies have reported that the efficacy of chemotherapy in treating glioma would be markedly improved if the therapeutic agent can be found that can pass through the BTB and BBB (23). These results suggested that $GdCl_3$ can accumulate and be uptaken by tumors in the brain through favorable permeability of the BTB and BBB. In addition, Gd compounds possess diverse anticancer activities (8,11). Previous studies have shown that after treatment with a relatively low concentration of $GdCl_3$, cell cycle progression and cell growth were promoted, whereas human hepatoma HepG2 and osteosarcoma U-2 OS cells exposed to high concentrations of $GdCl_3$ exhibited apoptosis and suppressed cell proliferation (8,11). It is suggested that $GdCl_3$-induced apoptosis is specific to HepG2 cells (11), U-2 OS cells (8) and rat C6 glioma cells. In this study, we demonstrated that $GdCl_3$ caused anti-proliferative effects on rat C6 glioma cells in a concentration-dependent manner (Fig. 1A). Our data demonstrated that the half-maximal inhibitory concentration (IC_{50}) values for a 24-h treatment of $GdCl_3$ in U-2 OS and rat C6 glioma cells were 198.26±1.69 and 152.36±2.45 μM, respectively. In addition, Shen *et al* (24) and Fu *et al* (25) demonstrated that Gd promoted cell proliferation in mouse embryo fibroblast NIH3T3 cells. Ferreira *et al* (26) indicated that no effect was noted in regards to the viability of Kupffer cells after $GdCl_3$ exposure. Our data also revealed that there was no viability impact (Fig. 1C) and morphological change (data not shown) on $GdCl_3$-treated normal SVG p12 cells, suggesting that $GdCl_3$ has an extremely low toxicity in normal glial cells.

Apoptosis (type I programmed cell death) is a vital mechanism in antitumor drugs and cancer therapies (27,28). It is a promising approach to induce apoptosis in glioma. Induction of tumor cell apoptosis is one of the best strategies for treating glioma and multiple types of cancers (27,28). Apoptotic death can be activated by three main pathways (17,29). The extrinsic pathway is triggered through binding of extrinsic signals to death receptors, which leads to activation of caspase-8 (29,30). The mitochondrial (intrinsic signaling) pathway is activated upon cellular stresses such as ROS production and $\Delta\Psi m$ disruption, and this results in activation of caspase-9. Both the extrinsic and intrinsic pathways can activate caspase-3 signaling and the major executioner caspase cascade (16,29,31). Therefore, induction of apoptotic pathways by a novel agent is a potentially powerful approach to fighting cancer cells (32,33).

Our results indicate that a high concentration of $GdCl_3$ caused the apoptosis of C6 cells (Fig. 1). This is the first study to report that $GdCl_3$ could be successfully applied to promote cell death in rat C6 glioma cells. In the present study, an increase of DNA damage and fragmentation of cells (an apoptotic characteristic) was demonstrated after exposure to $GdCl_3$ (Fig. 2). Previous studies have shown that Gd^{3+} caused distinct effects depending on the type of target cells (8,11). $GdCl_3$ was

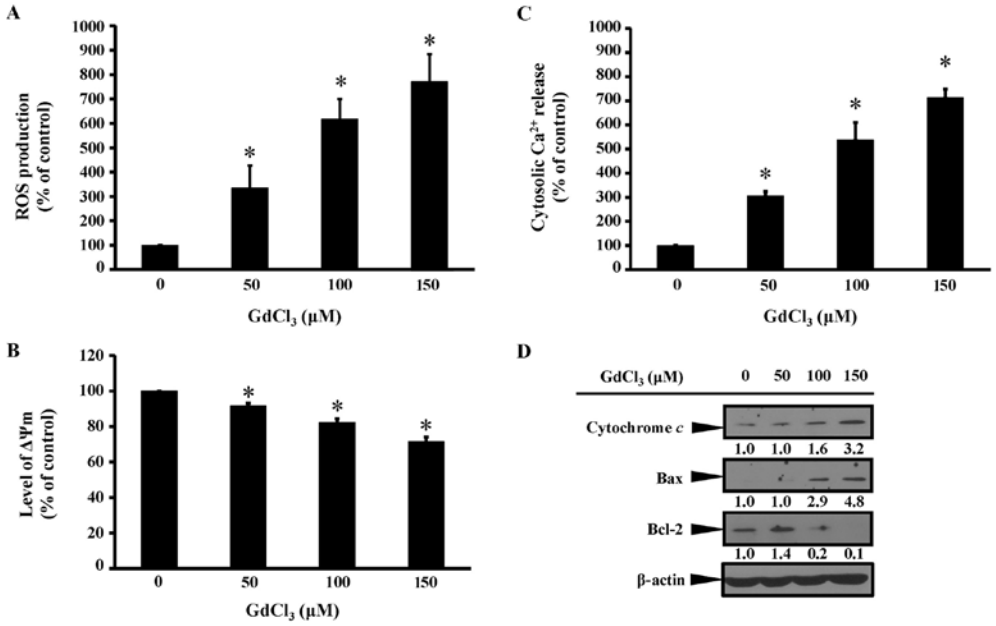

Figure 5. Effects of $GdCl_3$ on ROS production, ΔΨm, and cytoplasmic Ca^{2+} level of rat glioma C6 cells. Cells were treated with 50, 100, and 150 μM of $GdCl_3$ for 24 h. Cells were then mixed with (A) 5 μM dihydrorhodamine 123 for detecting ROS levels, (B) 4 nM fluorochrome DiOC6(3) for detecting the disruption of ΔΨm, and (C) 3 μg/ml Fluo-3/AM for detecting intracellular Ca^{2+} levels. MFI was measured by flow cytometry. Data are expressed as the mean ± SD (n=3). *P<0.05 compared to the control. (D) Immunoblotting analysis against cytochrome *c*, Bax, and Bcl-2 signals after $GdCl_3$ challenge for 24 h. β-actin was used as a loading control. Representative chemiluminescent images were collected from one of independent duplicate experiments. ROS, reactive oxygen species; $GdCl_3$, gadolinium chloride; ΔΨm, mitochondrial membrane potential; MFI, mean fluorescence intensity; SD, standard deviation.

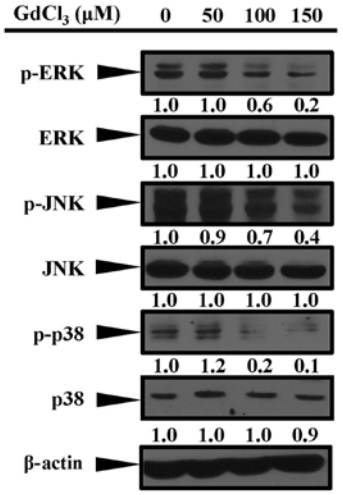

Figure 6. Effect of $GdCl_3$ on the levels of phosphorylation of MAPK signaling molecules in rat glioma C6 cells. Cells were exposed to 0, 50, 100, and 150 μM of $GdCl_3$ for 24 h. Cell fractions were extracted and subjected to immunoblotting analysis using the specific antibodies (p-ERK, ERK, p-JNK, JNK, p-p38 MAPK, and p38 MAPK). β-Actin was used as a loading control. Representative chemiluminescent images were collected from one of independent duplicate experiments. $GdCl_3$, gadolinium chloride; p-ERK, phosphorylated-extracellular signal-regulated kinase; p-JNK, phosphorylated-c-Jun N-terminal kinase; p-p38, phosphorylated-p38.

found to exert a proliferation-promoting ability and to activatee ERK and phosphoinositide 3-kinase (PI3K) signaling pathways in NIH 3T3 cells (24). Gd triggered cell apoptosis through the mitochondrial pathway in human osteosarcoma U-2 OS cells (8). Therefore, we sought to investigate the exact effect of $GdCl_3$ on cell proliferation and cell apoptosis in rat C6 glioma cells.

Apoptosis can be induced though activation of a cascade of caspases (29,31). Ye *et al* (11) showed that $GdCl_3$ triggered HepG2 cell apoptosis through death receptor-dependent and mitochondrial pathways. Our findings previously reported that $GdCl_3$-induced apoptosis may be mediated through the extrinsic pathway, the intrinsic pathway, and the ER stress pathway in human osteosarcoma U-2 OS cells (8). Caspase-3 (a 35-kDa protein), a critical executioner of apoptosis, is either partially or totally responsible for the proteolytic cleavage by nuclear enzyme poly (ADP-ribose) polymerase (PARP) (34). Activation of caspase-3 requires proteolytic processing of its inactive zymogen into activated p17 fragments. Caspase-8 is a 55-kDa protein and is an inactive pro-enzyme. Activation of caspase-8 involves a two-step proteolysis: i) the cleavage of caspase-8 to generate a 43- and a 12-kDa fragment which is further processed to 10 kDa; and ii) p43 is then cleaved to yield p26 and the release of the active site containing p18 (35-37). Caspase-9 is an important family protein in the intrinsic apoptotic pathway (38). Upon apoptotic stimulation, cytochrome c released from mitochondria associates with the 47-kDa procaspase-9/Apaf-1. Apaf-1-mediated activation of caspase-9 involves intrinsic proteolytic processing resulting in cleavage on Asp315 and producing a p35 subunit. Another cleavage occurs on Asp330 producing a p37 subunit that can serve to amplify the apoptotic response (39-41). In this study, $GdCl_3$ increased the enzymatic activities of caspase-3, caspase-8, and caspase-9, as well as cleaved-caspase-3 (p19), cleaved-caspase-8 (p18), and cleaved-caspase-9 (p35) protein levels *in vitro* (Fig. 3). Our results suggested that $GdCl_3$-triggered apoptosis of C6 cells resulted from caspase-dependent signaling. Furthermore, $GdCl_3$ elevated the ROS production and decreased the levels

of ΔΨm (Fig. 5). The expression level of the anti-apoptotic protein Bcl-2 was decreased, while the expression levels of cytochrome c and pro-apoptotic protein Bax were increased after $GdCl_3$ exposure in C6 cells (Fig. 5D). Our results found that $GdCl_3$-triggered apoptosis of C6 cells was mitochondria-dependent.

The influx of Ca^{2+} is involved in several biological functions including cell proliferation, apoptosis and differentiation (42,43). Ca^{2+} rapidly flows into the cytoplasm and into the mitochondria, leading to cell apoptosis (29,31). Xia *et al* (44) demonstrated that Gd caused oxidative stress in rat cortical neurons. Feng *et al* (45) indicated that Gd triggered ER stress and unfolded protein responses in primary cultured rat cortical astrocytes through an increase in the influx of extracellular Ca^{2+} level. However, no report regarding $GdCl_3$-induced ER stress in rat C6 glioma cells has been conducted. The present study revealed that $GdCl_3$ caused the release of Ca^{2+}, which led to apoptosis in C6 cells (Fig. 5C). Thus, our results suggest that $GdCl_3$-induced cell death may be mediated via the apoptotic mechanism in C6 cells.

MAPKs are divided into three main subfamilies: ERK, JNK, and p38 MAPKs. Increasing evidence has shown that MAPKs play crucial roles and exhibit cell functions in cell survival, cell proliferation, cell cycle regulation, and apoptotic death (46,47). ERK is involved in cell survival, and JNK and p38 MAPK are thought to mainly promote cell apoptosis (48,49). Activation of ERK1/2 has been demonstrated to inhibit apoptosis in response to tumor necrosis factor (TNF), Fas ligand, radiation, stress, hypoxia, and chemotherapeutic agent stimulation (50). Subramanian *et al* (51) suggested that estrogen-induced increase in Ca^{2+} leads to ERK phosphorylation and consequently CREB phosphorylation, resulting in an increase in the anti-apoptotic Bcl-2 protein level. The inactivation of pro-apoptotic Bcl-2 family member BAD is mediated through phosphorylation on Ser112 by ERK activated p90 ribosomal S6 kinase (RSK). Inhibition of JNK2 activity can also suppress tumorigenesis by promoting apoptosis (52). Yu *et al* (53) demonstrated that one of the molecular mechanisms by which JNK suppresses apoptosis is through phosphorylation of BAD on Thr201, thereby inhibiting its pro-apoptotic activity. p38 plays a role in cell survival supported by increased levels of Bcl-2 and Bcl-xL in response to DNA damage and stress (54,55). Furthermore, the chemical inhibition of p38 has been strongly associated with increased chemosensitivity in tumor cells (56,57). Intriguingly, in this study, the expression of p-ERK, p-JNK, and p-p38 MAPKs were downregulated after $GdCl_3$ exposure (Fig. 6). MAPKs were crucial for $GdCl_3$-induced apoptosis in C6 cells. We suggest that the phosphorylation of MAPKs was involved in Bcl-2 modulation in $GdCl_3$-induced apoptosis of C6 cells. Wang *et al* (58) demonstrated that $GdCl_3$ inhibits PC3 cell migration by the inactivation of both ERK and p38 MAPK pathways. Our results are in accordance with that study (58), which indicated that $GdCl_3$ suppressed ERK and p38 MAPKs and triggered apoptosis in C6 glioma cells.

In conclusion, $GdCl_3$ provoked apoptosis in C6 cells through upregulation of cytochrome *c* and Bax, downregulation of Bcl-2, and activation of caspase-3, caspase-8, and caspase-9 signaling. $GdCl_3$ triggered C6 cell apoptosis via mitochondria-dependent pathway. $GdCl_3$ may be a promising therapy for human glioma and an adjunct to other chemotherapies. Our findings provide a new molecular mechanism underlying the action of $GdCl_3$ for the chemotherapy of glioma.

Acknowledgements

Not applicable.

Funding

The present study was supported by the Shin-Kong Wu Ho-Su Memorial Hospital (Taipei, Taiwan (grant no. SKH-8302-106-DR-26) and in part by China Medical University Hospital (Taichung, Taiwan) (grant no. DMR-107-137).

Availability of data and materials

The datasets generated during the study are available from the corresponding author on reasonable request.

Authors' contributions

YFT, SCT and JSY conceived and designed the experiments. YFC, CYH, CWH and CCL performed the experiments. CCL, SCT and JSY analyzed the data. YFT, SCT and JSY wrote and modified the study. All authors read and approved the manuscript and agree to be accountable for all aspects of the research in ensuring that the accuracy or integrity of any part of the study are appropriately investigated and resolved.

Ethics approval and consent to participate

Not applicable.

Patient consent for publication

Not applicable.

Competing interests

The authors declare that they have no competing interests.

References

1. Miranda A, Blanco-Prieto M, Sousa J, Pais A and Vitorino C: Breaching barriers in glioblastoma. Part I: Molecular pathways and novel treatment approaches. Int J Pharm 531: 372-388, 2017.
2. Perry A and Wesseling P: Histologic classification of gliomas. Handb Clin Neurol 134: 71-95, 2016.
3. Sanai N and Berger MS: Surgical oncology for gliomas: The state of the art. Nat Rev Clin Oncol 15: 112-125, 2018.
4. Nam JY and de Groot JF: Treatment of Glioblastoma. J Oncol Pract 13: 629-638, 2017.
5. Dréan A, Goldwirt L, Verreault M, Canney M, Schmitt C, Guehennec J, Delattre JY, Carpentier A and Idbaih A: Blood-brain barrier, cytotoxic chemotherapies and glioblastoma. Expert Rev Neurother 16: 1285-1300, 2016.
6. Zhan C and Lu W: The blood-brain/tumor barriers: Challenges and chances for malignant gliomas targeted drug delivery. Curr Pharm Biotechnol 13: 2380-2387, 2012.
7. Zhao YY, Yang R, Xiao M, Guan MJ, Zhao N and Zeng T: Kupffer cells activation promoted binge drinking-induced fatty liver by activating lipolysis in white adipose tissues. Toxicology 390: 53-60, 2017.

8. Tsai YF, Huang CW, Chiang JH, Tsai FJ, Hsu YM, Lu CC, Hsiao CY and Yang JS: Gadolinium chloride elicits apoptosis in human osteosarcoma U-2 OS cells through extrinsic signaling, intrinsic pathway and endoplasmic reticulum stress. Oncol Rep 36: 3421-3426, 2016.
9. Wu Y, Wang Y, Li M, Yang X, Gong J and Zhang W: Gadolinium chloride suppresses acute rejection and induces tolerance following rat liver transplantation by inhibiting Kupffer-cell activation. Exp Ther Med 8: 1777-1782, 2014.
10. Hou CC, Feng M, Wang K and Yang XG: Lanthanides inhibit adipogenesis with promotion of cell proliferation in 3T3-L1 preadipocytes. Metallomics 5: 715-722, 2013.
11. Ye L, Shi Z, Liu H, Yang X and Wang K: GdCl3 induced Hep G2 cell death through mitochondrial and external death pathways without significant elevation of ROS generation. Biol Trace Elem Res 151: 148-155, 2013.
12. Yan L, Zhu TB, Wang LS, Pan SY, Tao ZX, Yang Z, Cao K and Huang J: Inhibitory effect of hepatocyte growth factor on cardiomyocytes apoptosis is partly related to reduced calcium sensing receptor expression during a model of simulated ischemia/reperfusion. Mol Biol Rep 38: 2695-2701, 2011.
13. Yang K, Du C, Cheng Y, Li Y, Gong J and Liu Z: Augmenter of liver regeneration promotes hepatic regeneration depending on the integrity of Kupffer cell in rat small-for-size liver transplantation. J Surg Res 183: 922-928, 2013.
14. Lu CC, Yang JS, Chiang JH, Hour MJ, Lin KL, Lee TH and Chung JG: Cell death caused by quinazolinone HMJ-38 challenge in oral carcinoma CAL 27 cells: dissections of endoplasmic reticulum stress, mitochondrial dysfunction and tumor xenografts. Biochim Biophys Acta 1840: 2310-2320, 2014.
15. Chiang JH, Yang JS, Lu CC, Hour MJ, Liu KC, Lin JH, Lee TH and Chung JG: Effect of DNA damage response by quinazolinone analogue HMJ-38 on human umbilical vein endothelial cells: evidence for γH2A.X and DNA-PK-dependent pathway. Hum Exp Toxicol 33: 590-601, 2014.
16. Chang CH, Lee CY, Lu CC, Tsai FJ, Hsu YM, Tsao JW, Juan YN, Chiu HY, Yang JS and Wang CC: Resveratrol-induced autophagy and apoptosis in cisplatin-resistant human oral cancer CAR cells: A key role of AMPK and Akt/mTOR signaling. Int J Oncol 50: 873-882, 2017.
17. Chang HP, Lu CC, Chiang JH, Tsai FJ, Juan YN, Tsao JW, Chiu HY and Yang JS: Pterostilbene modulates the suppression of multidrug resistance protein 1 and triggers autophagic and apoptotic mechanisms in cisplatin-resistant human oral cancer CAR cells via AKT signaling. Int J Oncol: Mar 2, 2018 (Epub ahead of print).
18. Chiu YJ, Hour MJ, Jin YA, Lu CC, Tsai FJ, Chen TL, Ma H, Juan YN and Yang JS: Disruption of IGF-1R signaling by a novel quinazoline derivative, HMJ-30, inhibits invasiveness and reverses epithelial-mesenchymal transition in osteosarcoma U-2 OS cells. Int J Oncol: Mar 16, 2018 (Epub ahead of print).
19. Lu CC, Yang JS, Huang AC, Hsia TC, Chou ST, Kuo CL, Lu HF, Lee TH, Wood WG and Chung JG: Chrysophanol induces necrosis through the production of ROS and alteration of ATP levels in J5 human liver cancer cells. Mol Nutr Food Res 54: 967-976, 2010.
20. Jensen RL: Brain tumor hypoxia: Tumorigenesis, angiogenesis, imaging, pseudoprogression, and as a therapeutic target. J Neurooncol 92: 317-335, 2009.
21. Liu Y, Hashizume K, Samoto K, Sugita M, Ningaraj N, Asotra K and Black KL: Repeated, short-term ischemia augments bradykinin-mediated opening of the blood-tumor barrier in rats with RG2 glioma. Neurol Res 23: 631-640, 2001.
22. Robert P, Frenzel T, Factor C, Jost G, Rasschaert M, Schuetz G, Fretellier N, Boyken J, Idée JM and Pietsch H: Methodological aspects for preclinical evaluation of gadolinium presence in brain tissue: critical appraisal and suggestions for harmonization-a joint initiative. Invest Radiol 53: 499-517, 2018.
23. Fitzgerald RT, Agarwal V, Hoang JK, Gaillard F, Dixon A and Kanal E: The impact of gadolinium deposition on radiology practice: an international survey of radiologists. Curr Probl Diagn Radiol S0363-0188(17)30296-7, 2018.
24. Shen L, Yang A, Yao P, Sun X, Chen C, Mo C, Shi L, Chen Y and Liu Q: Gadolinium promoted proliferation in mouse embryo fibroblast NIH3T3 cells through Rac and PI3K/Akt signaling pathways. Biometals 27: 753-762, 2014.
25. Fu LJ, Li JX, Yang XG and Wang K: Gadolinium-promoted cell cycle progression with enhanced S-phase entry via activation of both ERK and PI3K signaling pathways in NIH 3T3 cells. J Biol Inorg Chem 14: 219-227, 2009.
26. Ferreira J, Tapia G and Videla LA: Effects of the Kupffer cell inactivator gadolinium chloride on rat liver oxygen uptake and content of mitochondrial cytochromes. FEBS Lett 426: 263-265, 1998.
27. Bögler O and Weller M: Apoptosis in gliomas, and its role in their current and future treatment. Front Biosci 7: e339-e353, 2002.
28. Steinbach JP and Weller M: Apoptosis in gliomas: Molecular mechanisms and therapeutic implications. J Neurooncol 70: 245-254, 2004.
29. Yang JS, Lu CC, Kuo SC, Hsu YM, Tsai SC, Chen SY, Chen YT, Lin YJ, Huang YC, Chen CJ, *et al*: Autophagy and its link to type II diabetes mellitus. Biomedicine (Taipei) 7: 8, 2017.
30. Yuan CH, Horng CT, Lee CF, Chiang NN, Tsai FJ, Lu CC, Chiang JH, Hsu YM, Yang JS and Chen FA: Epigallocatechin gallate sensitizes cisplatin-resistant oral cancer CAR cell apoptosis and autophagy through stimulating AKT/STAT3 pathway and suppressing multidrug resistance 1 signaling. Environ Toxicol 32: 845-855, 2017.
31. Pfeffer CM and Singh ATK: Apoptosis: A Target for anticancer therapy. Int J Mol Sci 19: 19, 2018.
32. Lin C, Tsai SC, Tseng MT, Peng SF, Kuo SC, Lin MW, Hsu YM, Lee MR, Amagaya S, Huang WW, *et al*: AKT serine/threonine protein kinase modulates baicalin-triggered autophagy in human bladder cancer T24 cells. Int J Oncol 42: 993-1000, 2013.
33. Tsai SC, Yang JS, Peng SF, Lu CC, Chiang JH, Chung JG, Lin MW, Lin JK, Amagaya S, Wai-Shan Chung C, *et al*: Bufalin increases sensitivity to AKT/mTOR-induced autophagic cell death in SK-HEP-1 human hepatocellular carcinoma cells. Int J Oncol 41: 1431-1442, 2012.
34. Fernandes-Alnemri T, Litwack G and Alnemri ES: CPP32, a novel human apoptotic protein with homology to Caenorhabditis elegans cell death protein Ced-3 and mammalian interleukin-1 beta-converting enzyme. J Biol Chem 269: 30761-30764, 1994.
35. Muzio M, Chinnaiyan AM, Kischkel FC, O'Rourke K, Shevchenko A, Ni J, Scaffidi C, Bretz JD, Zhang M, Gentz R, *et al*: FLICE, a novel FADD-homologous ICE/CED-3-like protease, is recruited to the CD95 (Fas/APO-1) death-inducing signaling complex. Cell 85: 817-827, 1996.
36. Boldin MP, Goncharov TM, Goltsev YV and Wallach D: Involvement of MACH, a novel MORT1/FADD-interacting protease, in Fas/APO-1- and TNF receptor-induced cell death. Cell 85: 803-815, 1996.
37. Fernandes-Alnemri T, Armstrong RC, Krebs J, Srinivasula SM, Wang L, Bullrich F, Fritz LC, Trapani JA, Tomaselli KJ, Litwack G, *et al*: In vitro activation of CPP32 and Mch3 by Mch4, a novel human apoptotic cysteine protease containing two FADD-like domains. Proc Natl Acad Sci USA 93: 7464-7469, 1996.
38. Duan H, Orth K, Chinnaiyan AM, Poirier GG, Froelich CJ, He WW and Dixit VM: ICE-LAP6, a novel member of the ICE/Ced-3 gene family, is activated by the cytotoxic T cell protease granzyme B. J Biol Chem 271: 16720-16724, 1996.
39. Liu X, Kim CN, Yang J, Jemmerson R and Wang X: Induction of apoptotic program in cell-free extracts: Requirement for dATP and cytochrome c. Cell 86: 147-157, 1996.
40. Li P, Nijhawan D, Budihardjo I, Srinivasula SM, Ahmad M, Alnemri ES and Wang X: Cytochrome c and dATP-dependent formation of Apaf-1/caspase-9 complex initiates an apoptotic protease cascade. Cell 91: 479-489, 1997.
41. Zou H, Li Y, Liu X and Wang X: An APAF-1.cytochrome c multimeric complex is a functional apoptosome that activates procaspase-9. J Biol Chem 274: 11549-11556, 1999.
42. Bhat TA, Chaudhary AK, Kumar S, O'Malley J, Inigo JR, Kumar R, Yadav N and Chandra D: Endoplasmic reticulum-mediated unfolded protein response and mitochondrial apoptosis in cancer. Biochim Biophys Acta Rev Cancer 1867: 58-66, 2017.
43. Bahar E, Kim H and Yoon H: ER Stress-mediated signaling: action potential and Ca (2+) as key players. Int J Mol Sci 17: 17, 2016.
44. Xia Q, Feng X, Huang H, Du L, Yang X and Wang K: Gadolinium-induced oxidative stress triggers endoplasmic reticulum stress in rat cortical neurons. J Neurochem 117: 38-47, 2011.
45. Feng X, Xia Q, Yuan L, Yang X and Wang K: Impaired mitochondrial function and oxidative stress in rat cortical neurons: implications for gadolinium-induced neurotoxicity. Neurotoxicology 31: 391-398, 2010.
46. Eblen ST: Extracellular-regulated kinases: signaling from Ras to ERK substrates to control biological outcomes. Adv Cancer Res 138: 99-142, 2018.

47. Faghfuri E, Nikfar S, Niaz K, Faramarzi MA and Abdollahi M: Mitogen-activated protein kinase (MEK) inhibitors to treat melanoma alone or in combination with other kinase inhibitors. Expert Opin Drug Metab Toxicol 14: 317-330, 2018.
48. Gkouveris I and Nikitakis NG: Role of JNK signaling in oral cancer: A mini review. Tumour Biol 39: 1010428317711659, 2017.
49. Peluso I, Yarla NS, Ambra R, Pastore G and Perry G: MAPK signalling pathway in cancers: Olive products as cancer preventive and therapeutic agents. Semin Cancer Biol: Sep 11, 2017 (Epub ahead of print).
50. Lu Z and Xu S: ERK1/2 MAP kinases in cell survival and apoptosis. IUBMB Life 58: 621-631, 2006.
51. Subramanian M and Shaha C: Up-regulation of Bcl-2 through ERK phosphorylation is associated with human macrophage survival in an estrogen microenvironment. J Immunol 179: 2330-2338, 2007.
52. Potapova O, Anisimov SV, Gorospe M, Dougherty RH, Gaarde WA, Boheler KR and Holbrook NJ: Targets of c-Jun NH (2)-terminal kinase 2-mediated tumor growth regulation revealed by serial analysis of gene expression. Cancer Res 62: 3257-3263, 2002.
53. Yu C, Minemoto Y, Zhang J, Liu J, Tang F, Bui TN, Xiang J and Lin A: JNK suppresses apoptosis via phosphorylation of the proapoptotic Bcl-2 family protein BAD. Mol Cell 13: 329-340, 2004.
54. Flacke JP, Kumar S, Kostin S, Reusch HP and Ladilov Y: Acidic preconditioning protects endothelial cells against apoptosis through p38- and Akt-dependent Bcl-xL overexpression. Apoptosis 14: 90-96, 2009.
55. Kim MJ, Choi SY, Park IC, Hwang SG, Kim C, Choi YH, Kim H, Lee KH and Lee SJ: Opposing roles of c-Jun NH2-terminal kinase and p38 mitogen-activated protein kinase in the cellular response to ionizing radiation in human cervical cancer cells. Mol Cancer Res 6: 1718-1731, 2008.
56. Hamanoue M, Sato K and Takamatsu K: Inhibition of p38 mitogen-activated protein kinase-induced apoptosis in cultured mature oligodendrocytes using SB202190 and SB203580. Neurochem Int 51: 16-24, 2007.
57. Lim SJ, Lee YJ and Lee E: p38MAPK inhibitor SB203580 sensitizes human SNU-C4 colon cancer cells to exisulind-induced apoptosis. Oncol Rep 16: 1131-1135, 2006.
58. Wang P, Zou XM, Huang J, Zhang TL and Wang K: Gadolinium inhibits prostate cancer PC3 cell migration and suppresses osteoclast differentiation in vitro. Cell Biol Int 35: 1159-1167, 2011.